© UNIVERSAL RESEARCH REPORTS | REFEREED | PEER REVIEWED
ISSN : 2348 - 5612 | Volume : 05 , Issue : 02 | January – March 2018

Synthesis and photo luminescent properties of Dy^{3+} doped $BaZrO_3$ Nanophosphors

Sonika Singh[1], S.P. Khatkar[1], Rajesh Kumar[2], Sheetal[1], V.B. Taxak[1*]
[1]Department of Chemistry, Maharshi Dayanand University, Rohtak-124001, India
[2]Department of Applied Sciences, UIET, Maharshi Dayanand University, Rohtak-124001, India

Abstract : Dy^{3+} doped $BaZrO_3$ nanophosphors have been successfully synthesized via urea assisted solution combustion process. X-ray diffraction (XRD) and scanning electron microscopy (SEM)) were used to study the structural properties of Dy^{3+} doped $BaZrO_3$ nanophosphor. The XRD showd that $Ba_{1-x}Dy_xZrO_3$ nanophosphors crystallize in single cubic pervoskite structure having space group *P23* at 1200°C. SEM studies revealed cubical shaped particles having high agglomeration phenomenon with size distribution in nano range. Photoluminescent properties were studied by measuring excitation and emission spectra with decay curves of $Ba_{1-x}Dy_xZrO_3$ nanophosphors. The two main emission bands in the 470-490nm (blue region) centered at 482 nm and 560-580 nm (yellow region) centered at 575 nm corresponding to transitions of the Dy^{3+} ions from well-defined $^4F_{9/2}$energy states were observed. Luminescence concentration quenching could be observed when the doping concentration of Dysprosium ions was more than 3 mol%. Dy^{3+} doped $BaZrO_3$ nanophosphors could be potential optical material owing to their white light luminescence.

ISSN : 2348-5612 © URR
9 770234 856124

Keywords: Nanophosphor ● Combustion ● Photoluminescent ● $Ba_{1-x}Dy_xZrO_3$

Introduction : Barium zirconate having pervoskite–type structure possess an extraordinary potential for applications in different fields as thermal barrier coating (TBC) for supersonic air jets [1], material for interface engineering of alumina fiber composites [2-3] and proton conducting material in steam electrolyzer, humidity sensor and especially in solid oxide fuel cells (SOFCs) [4-6]. All these promising applications of this excellent refractory ceramic are attributed to its good mechanical strength, high thermal stability, low chemical reactivity with corrosive materials, high melting point (2600 ^oC) and low coefficient of thermal expansion ($\alpha = 87 \times 10^{-7}$ $/^oC$) [7-9]. $BaZrO_3$ has cubic structure belonging to *P23* (195) space group in which Zr atoms are bonded to six oxygen atoms forming octahedral ZrO_6 units while Ba atoms are bonded to 12 oxygen atoms in cuboctahedral manner as BaO_{12}. Within the ZrO_6 octahedron, zirconium atom resides in centrosymmetric positions [8].

Nowadays, intensive research has been made to explore potential of $BaZrO_3$ host matrix because doping of divalent or trivalent rare earth ions is quite easy in this single phased crystalline material. Rare earth (RE) doped barium zirconate is well known for light emission in the visible region via up-conversion or down-conversion mechanism. Several routes are reported in the literature including solid-state reaction, sol-gel, hydrothermal reaction, vapor phase synthesis and microwave assisted hydrothermal reaction for the synthesis of barium zirconate doped with different RE ion. Recently, Borja-Urby et al. [10] have exploited wet synthesis hydrothermal method to prepare Ce, Eu, Dy, Er, Yb doped $BaZrO_3$ phosphors. In the present report, Dy^{3+} doped $BaZrO_3$ nanophosphors have been synthesized adopting solution combustion synthesis (SCS) as well as their structural, morphological and luminescent features were also investigated in details. Solution combustion synthesis has been emerged as low cost, rapid and self sustained process which yields highly crystalline and homogenous oxide powders with large surface in a single step at lower temperature than the conventional synthesis method. Dy^{3+} ions show characteristic white light emission arising from appropriate yellow to blue (Y/B) emission ratio.

Influence of varying sintering temperature and dysprosium ions on $BaZrO_3$ nanophosphors has also taken in account in order to determine the exact optimal conditions for synthesizing these nanophosphors with superior luminescent properties.

A. EXPERIMENTAL

i) Powder Synthesis

$BaZr_{1-x}O_3$: xDy^{3+} nanophosphors were synthesized by solution combustion method using high purity $Ba(NO_3)_2.4H_2O$, ZrN_2O_7, $Dy(NO_3)_3.6H_2O$ and urea as starting reagents. The chemical equation for the reactions is:

$Ba(NO_3)_2 + xDy(NO_3)_3 + (1-x)ZrN_2O_7 + \sim 3.5\ CH_4N_2O \rightarrow BaZr_{1-x}Dy_xO_3$ (s) + gaseous products.

According to nominal composition of $BaZr_{1-x}O_3$: xDy^{3+} (x =0.01 to 0.05), a stoichiometric amount of metal nitrates were dissolved in minimum quantity of deionized water in 200 mL capacity pyrex beaker. Then urea was added in this solution with molar ratio of urea to oxidizer based on total oxidizing and reducing valencies of oxidizer and fuel (urea) according to concept used in propellant chemistry [11]. This aqueous paste containing calculated amount of metal nitrates and urea was then placed in a preheated furnace maintained at 500°C. The mixture of metal nitrates (oxidizers) and fuel (urea) undergo rapid and self-sustaining combustion process and the chemical energy released during this exothermic redox reaction results in dehydration and foaming followed by decomposition. Consequently, the large amounts of volatile combustible gases generated alongwith flames, yields voluminous solid within 5-8 minutes. The powders obtained were again fired from 800°C to 1200°C for 3h in order to increase brightness.

ii) Powder Characterization Techniques

The structural characterization of $BaZrO_3$: Dy^{3+} powders was done by high resolution X-ray diffraction (XRD) using Rigaku Ultima IV diffractometer with CuKα radiation at 40 kV tube voltage and 40 mA tube current in the 2θ range between 10-80°. The morphology of the particles was evaluated using Jeol JSM-6510 scanning electron microscope (SEM) The excitation and emission spectra of the phosphor were measured in the ultraviolet-visible region on Hitachi F-7000 fluorescence spectrophotometer with Xe-lamp at room temperature. The life time calculations of the phosphor were done by the software of the spectrophotometer (FL solution for F-7000).

B. RESULTS AND DISCUSSION

i) X-ray Studies

$BaZrO_3$ possess cubical perovskite structure where divalent 12-oxygen coordinated Ba cation resides in cuboctahedral site while 6-oxygen coordinated Zr atoms are present at centrosymmetric locations within the octahedron. XRD profiles of $BaZr_{0.97}Dy_{0.03}O_3$ nanophosphors as-synthesized and sintered at different temperatures alongwith the standard JCPDS No. 74-1299 are depicted in Fig.1a. All resolved diffraction peaks of $BaZr_{0.97}Dy_{0.03}O_3$ powder sintered at 1200°C, well matched the barium zirconate cubic phase (JCPDS No. 74-1299) having space group *P23* [195]. No additional peaks corresponding to the impurity phases were detected, indicating complete crystallization in single cubic pervoskite $BaZrO_3$ structure at this temperature. XRD profiles of $BaZr_{0.97}Dy_{0.03}O_3$ powder sintered at 800°C and 1100°C shows the presence of minor phase ZrO_2 (JCPDS No. 86-1499) along with diffraction peaks of main pervoskite phase. Although in as-synthesized $BaZr_{0.97}Dy_{0.03}O_3$ sample, weak reflex lines of unreacted nitrates were also apparent. However, it is quite noticeable that with the rise in temperature, peaks due to additional phases get diminished while intensity of main peak (110) enhanced with the decrease in full width half maximum (FWHM), indicating improvement in doping and crystallinity.

The XRD patterns of $BaZr_{(1-x)}Dy_xO_3$ powders sintered at 1200°C, doped with different contents of dysprosium ions alongwith the standard JCPDS No. 74-1299 are depicted in Fig. 1b. All the samples

crystallize in single cubic $BaZrO_3$ phase having space group *P23* [195], confirming no influence of small amount of Dy^{3+} ions on crystal structure of this lattice. The results also indicate that despite of ionic radii difference, Dy^{3+} (0.091nm) occupies Zr^{4+} (0.072nm) ion site as compared to larger Ba^{2+} (0.135nm) in $BaZrO_3$ host lattice [12]. The crystallite size, D of $BaZr_{(1-x)}Dy_xO_3$ powders was evaluated by Scherrer's formula, $D = 0.941\lambda/\beta \cos\theta$, where λ is the wavelength of CuKα radiation (0.1548 nm), β is the full width in radians at half-maximum (FWHM) and θ is the Bragg's angle of an observed. The calculated average crystallite sizes, by taking main peak (110) of $BaZr_{0.97}Dy_{0.03}O_3$ powders were found to be 9.7 nm, 24.0 nm. 29.4 nm and 43.5 nm at 500°C, 800°C, 1000°C and 1200°C, respectively. It can be observed from the calculated results as expected that with the increase of sintering temperature crystallite size also increases.

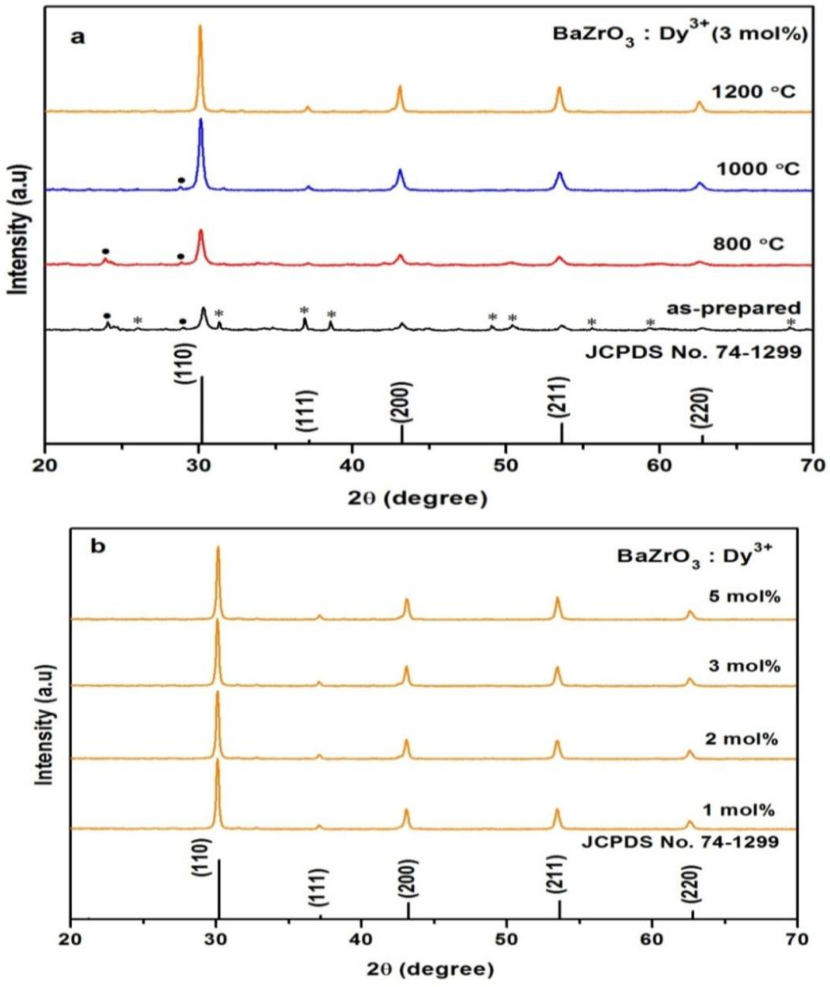

Fig.1. XRD patterns of (a) $BaZr_{0.97}Dy_{0.03}O_3$ powders sintered at various temperatures; (b) $BaZr_{(1-x)}Dy_xO_3$ (x =1 to 5 mol%) along with standard data of $BaZrO_3$ (JCPDS no. 74-1299)

ii) Morphological Studies

The SEM images of $BaZr_{0.97}Dy_{0.03}O_3$ powders$_3$ as sintered at temperatures 1000°C and 1200°C are represented in Fig. 2(a-b) respectively.

© UNIVERSAL RESEARCH REPORTS | REFEREED | PEER REVIEWED
ISSN : 2348 - 5612 | Volume : 05 , Issue : 02 | January – March 2018

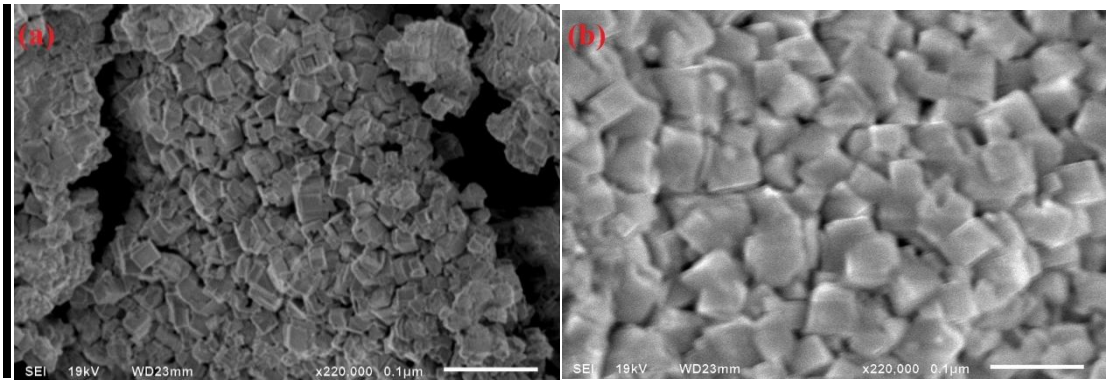

Fig .2. SEM images of $BaZr_{0.97}Dy_{0.03}O_3$ sintered at (a) 1000°C; (b) 1200°C.

For $BaZr_{0.97}Dy_{0.03}O_3$ sample sintered at 1000°C as shown in Fig. 2(a) cubical shaped particles having high agglomeration phenomenon are observed. Some voids and pores characteristic of combustion synthesized product are also apparent. With further rise of the sintering temperature upto 1200°C, clear morphology of tetragonal shape particles could be observed [13]. Hence, a uniform distribution of tetragonal particles having small size distribution is clearly visible in Fig. 2(b).

ii) Luminescent Studies

The photoluminescence excitation (PLE) spectrum of $BaZr_{0.97}Dy_{0.03}O_3$ nanophosphors, sintered at 1200°C, monitored with 575 nm ($^4F_{9/2} \rightarrow {}^6H_{13/2}$) as emission wavelength presented in Fig. 3. The PLE spectrum monitored at yellow emission comprised of several characteristic sharp peaks in 300 to 500 nm range corresponding to intra-4*f* transitions Dy^{3+} in the perovskite host. These excitation peaks in longer wavelength region at 327 nm, 354 nm, 366 nm, 389 nm, 429 nm, 453nm and 470 nm are assigned to $^6H_{15/2} \rightarrow {}^6P_{3/2}$, $^6H_{15/2} \rightarrow {}^6P_{7/2}$, $^6H_{15/2} \rightarrow {}^6P_{5/2}$, $^6H_{15/2} \rightarrow {}^4I_{13/2}$, $^6H_{15/2} \rightarrow {}^4G_{11/2}$, $^6H_{15/2} \rightarrow {}^4I_{15/2}$ and $^6H_{15/2} \rightarrow {}^4F_{9/2}$ transitions, respectively of Dy^{3+} ions in $BaZrO_3$ lattice [14]. In the short wavelength region, weak host or $O^{2-} \rightarrow Dy^{3+}$ charge sensitized luminescence indicates very weak Dy^{3+} ions interactions with perovskite host.

The photoluminescence (PL) spectra of $BaZr_{0.97}Dy_{0.03}O_3$ nanophosphor as-synthesized and sintered at different temperatures on monitoring excitation wavelength at 354 nm is depicted in Fig..4. The two main emission bands in the 470- 490nm (blue region) and 560-580 nm (yellow region) corresponding to transitions of the Dy^{3+} ions from well-defined $^4F_{9/2}$energy states were observed. The blue emission band centered at 482 nm is assigned to $^4F_{9/2} \rightarrow {}^6H_{15/2}$ while yellow emission band centered at 575 nm is ascribed to $^4F_{9/2} \rightarrow {}^6H_{13/2}$ transitions of Dy^{3+} ions, respectively [14-18]. All samples shows prominent hypersensitive forced electric transition (yellow emission) in as compared to magnetic dipole transition (blue emission) which gets hardly influenced by the crystal field symmetry of dysprosium ions. It is quite noticeable that rise in sintering temperature enhanced the relative PL intensity of as-synthesized $BaZr_{0.97}Dy_{0.03}O_3$ nanophosphors with maintained shape and positions of peaks corresponding to both transitions. This indicates that recombination defects and surface defects in perovskite lattice are omitted out after sintering of nanophosphors.

© UNIVERSAL RESEARCH REPORTS | REFEREED | PEER REVIEWED
ISSN : 2348 - 5612 | Volume : 05 , Issue : 02 | January – March 2018

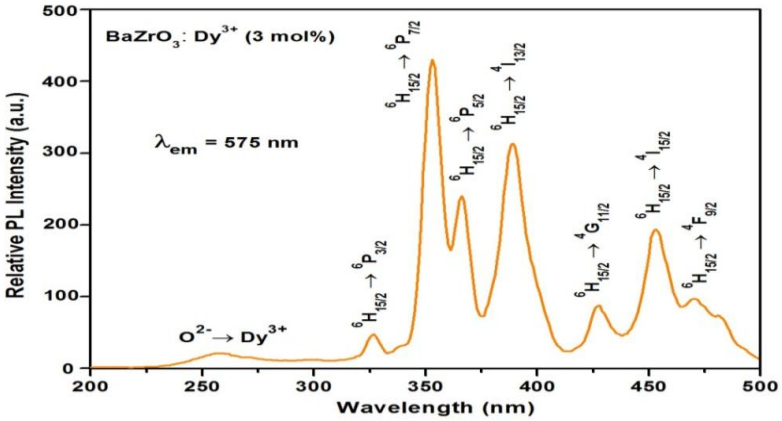

Fig .3. Photoluminescence excitation (PLE) spectrum of $BaZr_{0.97}Dy_{0.03}O_3$ nanophosphors, sintered at 1200°C, monitored with λ_{em} = 575 nm.

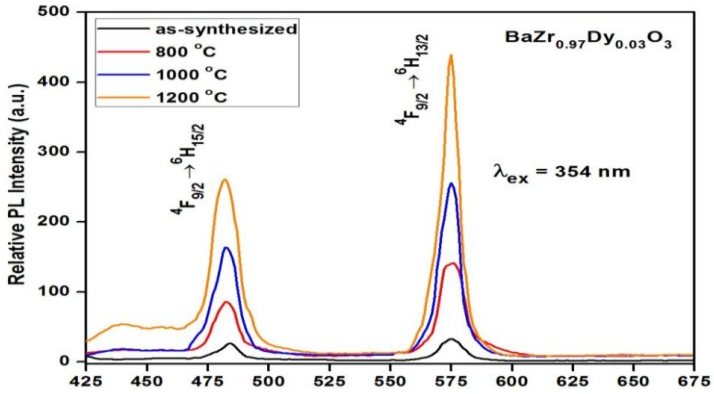

Fig. 4 Photoluminescence spectra (PL) of $BaZr_{0.97}Dy_{0.03}O_3$ nanophosphors, sintered at different temperatures, monitored with λ_{ex} = 354nm.

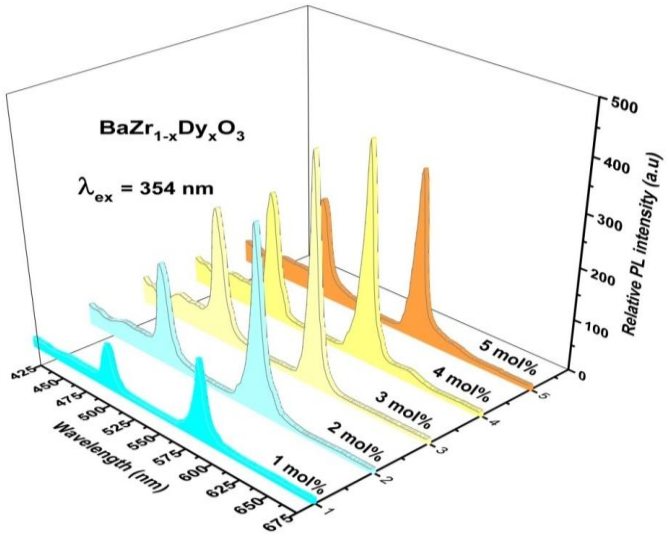

Fig. . Photoluminescence spectra of $BaZr_{1-x}Dy_xO_3$ nanophosphors with different Dy^{3+} contents, sintered at 1200°C and monitored with λ_{ex} = 354 nm.

The PL spectra of $BaZr_{1-x}Dy_xO_3$ nanophosphors, sintered at 1200°C with dysprosium doping contents ranging from 1 to 5 mol%, monitored with 354 nm as excitation wavelength are shown in Fig. 5. For all $BaZr_{1-x}Dy_xO_3$ samples, the hypersensitive yellow ($^4F_{9/2}\rightarrow{}^6H_{13/2}$) emission of Dy^{3+} ions is the prominent one while relative PL intensities corresponding to both yellow and blue emission enhanced with the increasing concentration of Dy^{3+} ions, reaching the maximum at 3 mol% of and decreased with the further increase of dopant contents. Non-radiative cross-relaxation mechanism between luminescent centers at higher dopant contents is primarily responsible for such kind of concentration quenching [19-20]. It has been noticed that value of yellow to blue emission ratio (Y/B ~1.6) has not been much influenced by varying dysprosium contents indicating that hypersensitive electric forced transition ($^4F_{9/2}\rightarrow{}^6H_{13/2}$) senses same crystal field environment at Dy^{3+} symmetry sites in $BaZrO_3$ lattice upto 5 mol%.

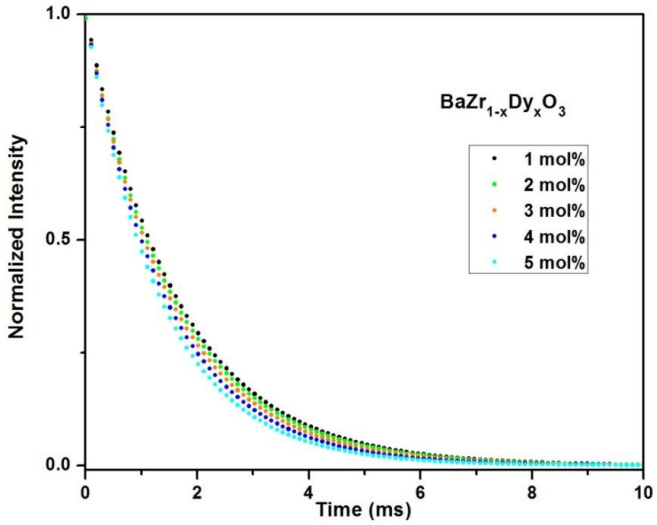

Fig. 6 Decay curves of $BaZr_{1-x}Dy_xO_3$ nanophosphors doped with different Dy^{3+}contents, sintered at 1200°C and monitored with λ_{ex} = 354 nm

The luminescence decay curves for $BaZr_{1-x}Dy_xO_3$ nanophosphors in terms of varying Dy^{3+} ions concentrations corresponding to prominent yellow emission at 575 nm, monitored with 354 nm excitation wavelength are displayed in Fig. 6. In all samples, $^4F_{9/2}\rightarrow{}^6H_{13/2}$ transitions show single exponential behavior, represented by the equation $I = I_0 \exp(-t/\tau)$, where τ is the radiative decay time, I and I_0 are the luminescence intensities at time t and 0, respectively. The calculated average lifetimes are 1.64, 1.60, 1.52, 1.44 and 1.35 for 1, 2, 3, 4, 5 mol% of Dy^{3+} ions, respectively.

The Commission International De I'Eclairage (CIE) color coordinates (x, y) calculated from the corresponding PL spectra of $BaZr_{1-x}Dy_xO_3$ nanophosphors, where x = 0.01 to 0.05 are displayed in Fig. 7. The Color coordinates for all $BaZr_{1-x}Dy_{x3}O_3$ samples lie in white region at (0.344, 0.362), (0.333, 0.358), (0.309, 0.332), (0.325, 0.331) and (0.333, 0.346) corresponding to 1, 2, 3, 4, and 5 mol%, respectively. Comparable value of color coordinates of these dysprosium doped nanophosphors to other standard color systems such as NTSC (0.3101, 0.3162), PAL/SECAM/HDTV (0.3127, 0.329), ProPhoto/Color Match (0.3457, 0.3585) and CIE white light point (0.33, 0.33), makes $BaZr_{1-x}Dy_xO_3$ nanophosphor an excellent candidate for white light emission in LEDs applications.

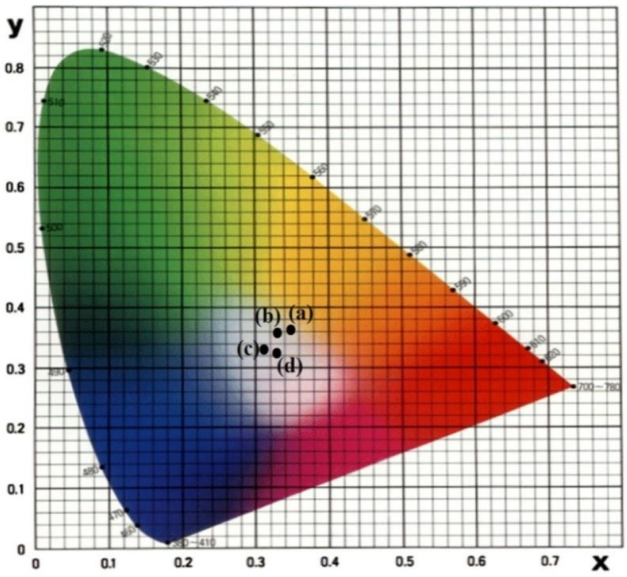

Fig. 7. CIE color (*x*, *y*) coordinates for (a) 1 mol%, (b) 2 mol%, (c) 3 mol%, and (d) 4 mol%, of Dy^{3+} ions in $BaZr_{1-x}Dy_xO_3$ nanophosphors sintered at 1200°C after excitation at 354 nm.

Conclusion

In summary, $BaZrO_3$: Dy^{3+} nanophosphors were successfully synthesized using combustion method. XRD result revealed that the particles sintered at 1200°C temperature crystallize in pure cubic phase. and their structural as well as luminescent characteristics were studied for various sintering temperature and dysprosium concentration. Highly crystalline single phased $Ba_{1-x}Dy_xZrO_3$ at 1200ºC as revealed by X-ray diffraction studies. Morphological studies showed narrow distribution of cubical particles in nano-regime. Luminescent features of Dy^{3+} doped $BaZrO_3$ nanophosphors were investigated using photoluminescence excitation (PLE) and photoluminescence emission (PL) alongwith luminescence decay curves and color (*x*, *y*) coordinates. In PL spectra, two sharp emission lines in the blue region and yellow region attributed to intra-4*f* transitions of the Dy^{3+} ions in 300-500 nm range were observed. Dy^{3+} doped $BaZrO_3$ nanophosphors exhibited maximum luminescence at 3 mol% of dysprosium ions.

References

1. R. Vassen, X. Cao, F. Tietz, D. Basu, D. Stover, *J. Am Ceram. Soc.*, 3 (200) 2023.
2. A. Erb, E. Walker, R. Flukiger, *Phys. C*, 245 ((1995) 245.
3. Z. Chen, S. Duncan, K.K. Chawla, M. Koopman, G.M. Janowski, *Mater. Charact.*, 48 (2002) 305.
4. H.G. Bohn and T. Schober, *J. Am Ceram. Soc.*, 83 (2000)768.
5. M. Viviani, M.T. Buscaglia, V. Buscagalia, M. Leoni, P. Nanni, *J. Eur. Ceram. Soc.*, 21 (2001) 1981.
6. K. Katahira, Y. Kohchi, T. Shiramura, H. Iwahara, *Solid State Ionics*, 138 (2001) 91.
7. H. Padma Kumar, C.V. Kumar, C.N. Geirge, S. Soloon, R. Jose, J.K. Thomas, J. Koshy, *J. Alloys Compds.*, 458 (20008) 528.
8. S. Parida, S.K. Rout, L.S. Cavalcante, E. Sinha, M.S. Li, V. Subramanian, N. Gupta, V.R. Gupta, J.A. Varela, E. Longo, *Ceram. Inter.*, 38 (2012) 2129.
9. M. Enhessari, S. Khanahmadzadeh, K. Ozaee, *J. Iran. Chem. Res.*,3 (2011) 11.
10. R. Borja-Urby, L.A. Diaz-Torres, P. Salas, C.Angeles-Chavez, O. Meza, *Mater. Sci. Engg. B*, 176 (2011) 1388.
11. S. Ekambaram and K.C. Patil, *J. Alloys Compds.*, 448 (1997) 7.

12. Sheetal Lohra, V. B. Taxak, Avni Khatkar, Sonika Singh, S.P. Khatkar, Opt. Quant. Electron., 46 (2014) 1499.
13. X.Q. Zeng, G.Y. Hong, H.P. You, X.Y. Chin, J. Lumin. 22 (2001) 58–63.
14. B. Tian, B. Chen, Y. Tian, J. Sun, X. Li, J. Zhang, H. Zhang, L. Cheng, R. Hua, *J. Chem. Phys. Solids*, 73 (2012)1314.
15. G.S.R. Raju, J.Y. Park, H.C. Jung, B.K. Moon, J.H. Jeong, J.H. Kim, *Curr. Appl. Phys.* 9 (2009) e92.
16. D. Gao, Y. Li, X. Lai, Y. Wei, J. Bi, Y. Li, M. Liu, *Mater. Chem. Phys.*, 126 (2011)391.
17. C.R. Kesavulu, and C.K. Jayasankar, *Mater. Chem. Phys.*, 130 (2011)1078.
18. C.H. Liang, L.G. Teoh, K.T. Liu, Y.S. Chang, *J. Alloys Compds.*, 517 (2012) 9.
19. S.D. Han, S.P. Khatkar, V.B. Taxak, G. Sharma, D. Kumar, *Mater. Sci. Eng. B*, 129 (2006)126.
20. L.A. Diaz-Torres, E.D.L. Rosa, P. Salas, V.H. Romero, A. Angeles-Chavez, *J. Solid State Chem.*, 181 (2008) 75.